Analysis of vibration exercise at varying frequencies by different fatigue estimators

Please check the document version of this publication:

Analysis of vibration exercise at varying frequencies by different fatigue estimators

Lin Xu, *Student Member, IEEE,* Chiara Rabotti, *Member, IEEE,* and Massimo Mischi, *Senior Member, IEEE*

Abstract—Vibration exercise (VE) has been suggested to improve muscle strength and power performance, due to enhanced neuromuscular demand. However, understanding of the most appropriate VE protocols is lacking, limiting the optimal use of VE in rehabilitation programs. In this study, the fatiguing effect of vibration at different frequencies was investigated by employing a force-modulation VE system. Twenty volunteers performed 12-s isometric contractions of the biceps brachii with a load consisting of a baseline force of 80% of their maximum voluntary contraction (MVC) and a superimposed sinusoidal force at 0 (control condition with no vibration), 20, 30, and 40 Hz. Mechanical fatigue was estimated by assessment of MVC decay after each task while myoelectric fatigue was estimated by analysis of multichannel EMG signals recorded during VE. EMG conduction velocity, spectral compression, power, and fractal dimension were estimated as indicators of myoelectric fatigue. Our results suggest vibration, in particular at 30 Hz, to produce a larger degree of fatigue as compared to control condition. These results motivate further research aiming at introducing VE in rehabilitation programs with improved training protocols.

Index Terms—Electromyography, Vibration exercise, Muscle fatigue, Conduction velocity, Fractal dimension.

I. INTRODUCTION

Vibration exercise (VE) has been reported to provide several important advantages over conventional strength training and has therefore been suggested as an alternative training modality to improve muscle strength and power performance [1], [2], [3]. Whole body vibration platforms have been suggested to be an effective modality to exercise the lower limbs and have become the most widely adopted vibration platforms [4], [5], [6], [7]. Alternative devices, such as vibrating dumbbells [1], vibrating barbells [8], and force-modulated vibration devices [9], [10], have also been proposed for the upper limbs.

The beneficial effects of VE in relation to muscle activation, strength, and power performance [1], [5], [9] have been associated with increased electromyography (EMG) activity observed during VE [1], [9], [11], which seems partly to be ascribed to a specific reflex mechanism named tonic vibration reflex (TVR) [12], [13], [14]. TVR is derived from the stimulation of Ia-afferents when a sinusoidal vibration is directly applied to a muscle or a tendon [13], [15], [16] and composed of motor unit activity synchronized and unsynchronized with the vibration cycle [17], [18]. Through TVR, muscles try to achieve vibration dampening and joint stiffening by preferential recruitment of faster motor units [13], [19]. In addition, TVR is also reported to be modulated by alterations in spindle sensitivity through γ feedback [13], [20]. However, studies have also suggested that TVR may contribute to muscle fatigue and/or increase the risk of cumulative trauma disorders observed after repetitive exposure of the hand to vibration [21].

Furthermore, it is reported that muscle response and adaptation to vibrating loads seem to be influenced by muscle contraction level [9], [14], [22]. Mischi and Cardinale [9] investigated how vibration affects muscle activation when superimposed to various levels of muscle tension and suggested that the effectiveness of such a modulation is clearly muscle-tension dependent. In addition, the vibration-induced increase in EMG activity and the degree of motor-unit synchronization seem also to be influenced by the characteristics of the input vibrating load, i.e., frequency and amplitude [5], [14], [23]. The VE frequencies adopted in previous studies were in the 15-60 Hz range [9], [23], [24]. However, the effect of different VE frequencies may differ for different muscles together with the optimal frequency to determine the best training stimulus.

Although several studies have been carried out, it is evident that a thorough understanding of the mechanisms and the neuromuscular responses involved in VE is still lacking, hampering the identification of the most appropriate vibration training protocols for rehabilitation programs. To better understand the neuromuscular responses to VE, the present study investigates the fatiguing effect of VE at different frequencies during sustained contraction, including mechanical fatigue and myoelectrical fatigue. To this end, a dedicated prototype realized in our previous study [25] was adopted that can apply a vibrating force to the muscle. Such a system has been shown to provide full control of the generated force, and vibration consists in a sinusoidal force modulation applied to the muscle. Twenty healthy volunteers were instructed to perform 12-s sustained isometric contractions of the biceps brachii. The adopted vibrating force was a superimposition of a baseline load corresponding to 80% of the maximum voluntary contraction (MVC) and a vibrating load with frequencies ranging from 0 (no vibration) to 40 Hz.

Mechanical fatigue was identified with the decay in force-production capability and assessed by MVC tests prior to and after each task. Myoelectric fatigue was assessed by analysing the EMG signals recorded during the 12-s isometric contraction. It is well reported that the power spectral density of the EMG signals undergoes compression towards lower frequencies during sustained contraction, resulting in a decrease in the MF [26], [27]. An increase in fatigue is also associated with an decrease in the motor unit conduction velocity (CV) along the muscle-fiber [26], [27]. The EMG root

L. Xu, C. Rabotti and M. Mischi are with the Faculty of Electrical Engineering, Eindhoven University of Technology, 5612 AZ, Eindhoven, The Netherlands (e-mail: l.xu@tue.nl).

mean square (RMS) value, being related to the mean power of the signal, is also found to increase with increasing fatigue during sustained contraction [28]. Recent studies indicated that the fractal dimension (FD) of the EMG signal decrease during fatiguing isometric contraction [29]. An estimate of the fatiguing effect of exercise can be derived as the angular coefficient of the linear fit of the MF, CV, RMS, and FD evolutions over time [26], [27], [29].

Several methods have been proposed for CV estimation in the literature, including calculation of the phase difference [30], [31], detection of spectral dips [32], [33], maximization of cross-correlation function [34], and estimation of the maximum likelihood (ML) [35], [36], [37]. The phase difference method is very sensitive to additive noise with respect to other techniques that use the same information [38]. For the use of the spectral dips method, one of the main issue is the large variance in the dip detection, which may be due to the variance of the estimated power spectrum [38]. The ML method, unlike the cross-correlation method, is implemented in the frequency domain, enabling CV estimation without resolution limitation due to the time-sampling rate [38]. Furthermore, the ML method, compared to the phase difference method, permits a complete exploitation of our multichannel measurements because it allows using all the available channels, leading to an increased robustness to a low signal to noise ratio. The ML method has, therefore, been adopted for the CV estimation in the present study.

In general, the EMG spectrum recorded during VE shows sharp peaks at the vibration frequency (SP_{VF}). In some studies, these SP_{VF} were considered as motion artifacts and excluded from the EMG analysis [2], [9], [39]. However, some other studies suggested those SP_{VF} to be vibration-induced muscle activity [14], [40], [41]. In the present study, in order to fairly examine the fatigue effect introduced by VE at different frequencies, estimation for the four fatigue indicators was performed under two conditions: with and without removing the SP_{VF}.

II. METHOD

A. Measurement setup

1) Actuator: The adopted actuator, whose scheme is shown in Fig. 1, has been described in detail elsewhere [25]. Briefly, an electrical motor generates a force consisting of a baseline force with superimposed sinusoidal force modulation. An example of such vibration force is given in Fig. 2. A planetary gearbox is connected to the motor, increasing the torque by a factor of 10 at the output shaft. A aluminium bar is connected to this shaft to apply the generated force vertically to the subject via a strap and a handle. The position of the bar is monitored by a rotary encoder embedded in the motor, providing a visual feedback to the training subject. The input voltage to the motor driver is controlled by dedicated software implemented in LabView® (National Instruments, Austin, TX).

The relationship between the driving voltage to the motor and the generated force was calibrated by means of a load cell LCAE-35kg (Omega Engineering Inc., Stamford, CT,
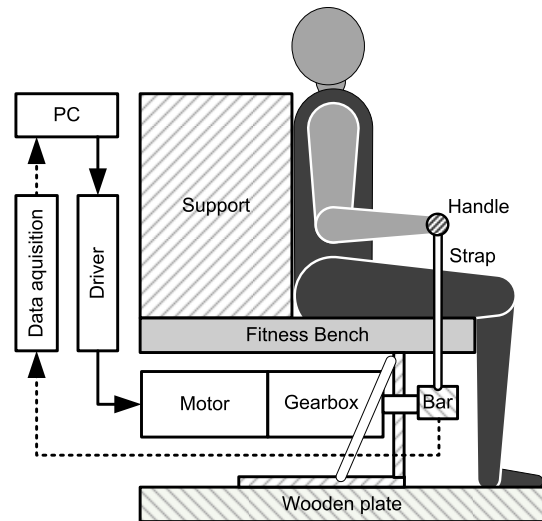
Fig. 1.   Scheme of the measurement setup.

USA), which uses resistance-based force sensors in full bridge configuration and is embedded in the aluminium bar [42]. The dedicated force calibration permitted applying to the muscle a well determined force, the same for all vibration frequencies. This step is essential to assess the fatiguing effects of different vibration frequencies.

2) EMG recording: Surface EMG was recorded from the biceps during each experimental trial using a high-density electrode grid, which consists of 8×8 contact Ag-AgCl electrodes with diameter of 2 mm and inter-electrode distance of 4 mm. The electrode grid was placed between the tendon at the elbow side and the muscle belly, with its columns aligned with the muscle fibers, as shown in Fig. 3. This position, distant from the muscle fiber innervation zone, enabled the EMG CV estimation by detecting a single propagation direction of the action potentials. The detected EMG signals were acquired by a 64-channel Refa® amplifier (TMS International, Enschede, the Netherlands) with a sampling frequency of 2048 Hz. Active shielding and grounding of the cables were used for reduction of the electromagnetic interference (50 Hz). The ground electrode was placed on top of the right clavicle.

Fig. 2.   Example of VE loading function: baseline with superimposed sinusoidal vibration.

Fig. 3. High-density electrode grid showing the muscle fiber orientation and the two sets of electrodes adopted for MF, RMS, and FD estimation.

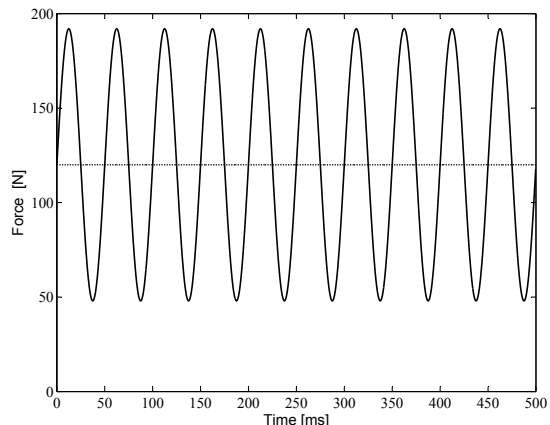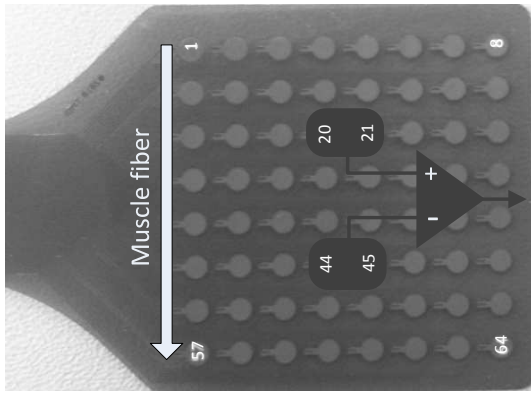### B. Subjects

Twenty male subjects (age $= 28 \pm 5$ years) volunteered for the experiment. All the subjects were right handed. They were healthy with no previous neurological disorder or injuries of the upper limbs. Written informed consent was obtained from every subject prior to participation in the study, and the test procedures were approved by the board of the Student Sport Centre of the Eindhoven University of Technology.

C. Measurement protocol

As shown in Fig. 1, subjects were seated on a bench above the actuator and hold the handle with their elbow at $90°$. Their back was supported in order to avoid shoulder movements which could influence the contraction of the biceps brachii. To maintain this gesture, the shaft position of the motor was monitored by the rotary encoder embedded in the actuator and was provided to the subject using a visual feedback displayed on a monitor. The MVC for each subject was then derived according to the following protocol. The subjects were instructed to pull the handle with 3-s maximal isometric contraction three times with a 1-min rest interval between each test. Preliminary dedicated measurements for the protocol design indicated this time interval to be adequate for the maximum force recovery. For each 3-s contraction, the maximum force was estimated based on the load cell output and the maximum of the three estimates was considered as the MVC.

After establishing the MVC, the subjects maintained the same position and performed 12-s isometric contractions. The force, applied by the actuator during the entire 12-s contraction, was the combination of a steady baseline force at 80% of the MVC and a superimposed sinusoidal force modulation with amplitude equal to 60% of the baseline (Fig. 2). Four trials were performed using a randomized cross-over design: with no vibration (control), and vibration at 20, 30, and 40 Hz. Each trial was followed by a recovery period of 12 minutes. Our dedicated measurements for the protocol design suggested 12-min to be adequate for muscle recovery while limiting the duration of the whole protocol. Multi-channel surface EMG were recorded during each 12-s trial. The MVC was also measured after each trial in order to estimate mechanical fatigue.

D. Signal processing

1) Data preprocessing: For the MF, RMS, and FD analysis, one single bipolar signal was extracted by taking the difference of the average EMG in two subsets of two electrodes, as shown in Fig. 3. For the CV estimation, all the EMG signals were first normalized to obtain zero mean and unit variance and then bipolarized along the muscle fiber by subtracting the adjacent electrodes signals in the same column, leading to 8 parallel columns of 7 bipolar signals. Fig. 4 shows an example of the bipolar signals recorded by one column of the electrode grid.

The derived EMG signals were first band-pass filtered between 20-450 Hz using a fourth-order Butterworth filter and then divided into adjacent 1-s, no-overlapping epochs for a total number of 12 epochs [43]. MF, CV, RMS, and FD were estimated for each epoch both with and without removing the SP_VF. For the estimation of MF, CV, and RMS, which can be calculated in the frequency domain, SP_VF removal was obtained by nulling the spectral components at the vibration frequency and its harmonics [9]. For the FD calculated in the time domain, the SP_VF were removed by notch filtering [2].

2) MF estimation: The MF was estimated as the first statistical moment of the Short-time Fourier Transform (STFT) amplitude spectrum,

$$\text{MF} = \frac{\sum_{f=20}^{450} f \cdot S_f}{\sum_{f=20}^{450} S_f}, \tag{1}$$

where f is the frequency [Hz] and S_f the amplitude spectrum at frequency f.

3) CV estimation: The progression of CV was estimated using the ML method described in [35], [37]. For the 8 (columns) $\times$ 7 (rows) bipolar EMG signals derived for CV estimation, we assume that signal x_{rc} from the rth row and c^{th} column is delayed by a number, θ, of samples relative to the previous row and embedded in additive, white, Gaussian
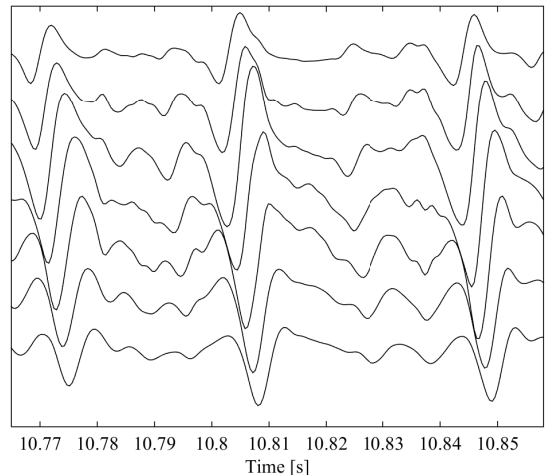

Fig. 4. Example of the EMG signals recorded by one column of the electrode grid with 30 Hz vibration.

noise $v_{rc}(n)$ with variance σ_{rc}^2. The multichannel signal model is then defined by

$$x_{rc}(n) = s_c[n - (r-1)\theta] + v_{rc}(n),$$
$$n = 1, ..., N; r = 1, ..., N_r; c = 1, ..., N_c \qquad (2)$$

where r is the indicator of rows, N_r the number of rows, c the indicator of columns, N_c the number of columns, N the number of samples, and $s_c(n)$ is the noise-free signal at column c. The CV was calculated by: $\text{CV} = d \cdot f_s / \theta$, where d is the inter-electrode distance and f_s the sampling frequency.

The CV calculation requires the estimation of θ, which can be obtained by the maximization of $p(\theta | \underline{x}_{11}, ..., \underline{x}_{N_r N_c}, \underline{s}_c)$, where $\underline{x}_{rc}$ and $\underline{s}_c$ are the vector representation of $x_{rc}(n)$ and $s_c(n)$, respectively. Using Bayesian inference and assuming $p(\theta)$ uniform, maximization of $p(\theta | \underline{x}_{11}, ..., \underline{x}_{N_r N_c}, \underline{s}_c)$ corresponds to the maximization of the multivariate Gaussian Probability Density Function (PDF) $p(\underline{x}_{11}, ..., \underline{x}_{N_r N_c} | \theta, \underline{s}_c)$ of the available observations. The ML estimation of θ is then given by (see appendix)

$$\hat{\theta} = arg \max_\theta \Big(\sum_{c=1}^{N_c} \sum_{r=1}^{N_r} \sum_{m=1}^{N_r}$$
$$\frac{1}{2\pi} \int_{-\pi}^{\pi} X_{rc}(e^{j\omega}) X_{mc}^*(e^{j\omega}) e^{j(r-m)\theta\omega} d\omega \Big), \quad (3)$$

where $*$ indicates the complex conjugate and $X_{rc}(e^{j\omega})$ and $X_{mc}(e^{j\omega})$ denote the STFT of $x_{rc}(n)$ and $x_{mc}(n)$, respectively, which are continuous-valued function of the angular frequency ω. In (3), θ no longer needs to be constrained to integer values but can be treated as continuous-valued.

To find the optimum value for θ, two search steps were performed. A first rough estimation of θ, $\hat{\theta}_1$, was obtained by finding the maximum value of the integral in (3) with θ ranging from 0.5 to 10 samples in steps of 0.5 sample. With the given inter-electrode distance of 4 mm and a sampling frequency of 2048 Hz, this search range of θ corresponds to CV ranging from 0.82 to 16.4 m/s, which fully covers the CV range reported in the literature for the biceps brachii [44], [45]. More accurate search of the maximum value of the integral in (3) was then performed in a small range ($\hat{\theta}_1 \pm 0.5$) in steps of 0.01. Given the adopted sampling frequency (2048 Hz), this step length leads to a resolution of 0.005 ms for the estimated delay.

4) RMS estimation: In order to perform fatigue estimation with SP_{VF} removal in the frequency domain, the RMS estimation was performed by using of Parseval's equality, as given by

$$\text{EMG}_{\text{RMS}} = \sqrt{\frac{1}{K} \sum_{k=1}^{K} |x[k]|^2} = \frac{1}{K} \sqrt{\sum_{k=1}^{K} |X[k]|^2}, \quad (4)$$

where $X[k]$ is the Fourier Transform of $x[k]$ and K the number of samples.

5) FD estimation: FD gives a quantitative indication of the chaotic behaviour of the signal. The box-counting method described in [46] was employed to estimate FD in this study. Fractals show an inverse power law relationship between the number of boxes required to cover the signal N and the box size L, as given by

$$N = L^{-FD}. \qquad (5)$$

To estimate FD, a set of square boxes with different sizes are used to cover the signal. The number of boxes required to cover the signal will increase exponentially as the box size decreases. An approximately linear relationship can be obtained by plotting the log of the number of boxes (log N) versus the log of the inverse of the box size (log l/L). The slope of the regression line is then the FD.

However, for nature fractal structures, this linear relationship exits only over a limited range of box sizes over which self similarity exits in the waveform. Therefore, the log N vs. log $1/L$ plots were first made in a wide range of box sizes (2-512) and the correct range of box sizes was then chosen to incorporate the region over which a linear relationship existed between log N and log $1/L$.

6) Fatigue estimation: Each myoelectric fatigue indicator was estimated in every 1-s epoch. Linear regression was then applied to the values obtained from all the epochs during each task and the slope of the regression line was used as the estimation for myoelectric muscle fatigue [47], [29]. Similar to previous studies [47], subject exclusion was performed based on the regression coefficient of MF and CV since they are reported to be much higher than that of RMS and FD [29], [47]. Subjects with MF or CV regression coefficient higher than 0.6 were included, resulting in 15 subjects for all the four fatigue indicators. For each indicator, the estimated slopes at different vibration frequencies for one subject were normalized with respect to the maximum decay (MF, CV, and FD) or increase (RMS) in order to reduce the bias caused by the differences among subjects. All the analysis was implemented in Matlab® (MathWorks, Natick, MA).

E. Statistical analysis

Statistical analysis was performed on both myoelectric fatigue and mechanical fatigue. Mechanical fatigue was estimated as the relative drop in MVC after each task. All data are presented as mean and SD. One sample Kolmogorov-Smirnov test suggested our data to be normally distributed [48]. Therefore, for each fatigue indicator, the effect of different vibration frequencies was examined globally by a one-way ANOVA, being each group represented by fatigue indicators at a given vibration frequency, and compared individually between each two groups by a post hoc test using Tukey's least significant difference procedure [49].

III. RESULTS

A. MF estimation

MF was first estimated after removing the SP_{VF}. The initial MFs for each subjects, estimated at the first epoch of different trials, are shown in Fig. 5 (a). The average value of all
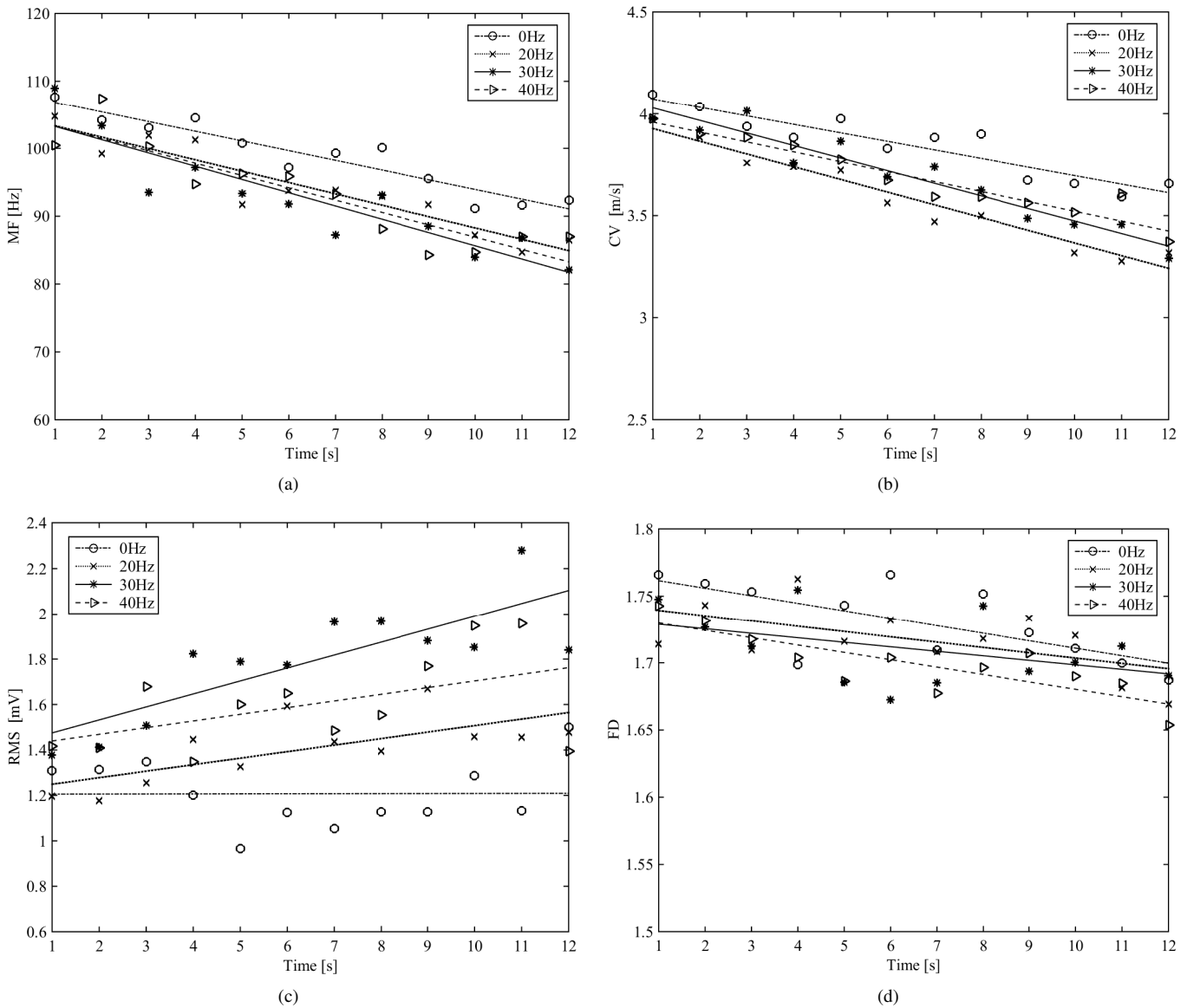
Fig. 6. Example of MF (a), CV (b), RMS (c), and FD (d) estimates for subsequent epochs at varying vibration frequencies.
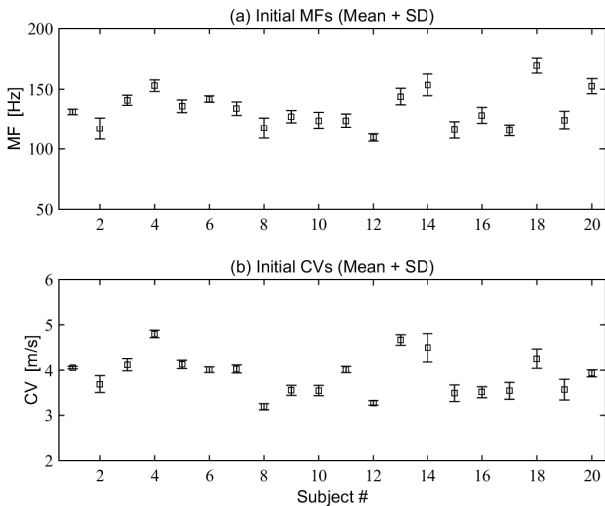
Fig. 5. Initial MFs and CVs for each subjects, estimated at the first epoch of different trials.

estimates were 120 ± 16 Hz, which is in the range reported in the literature for the biceps brachii [44]. A linear regression was then applied to the estimates obtained from all the epochs during each task. Fig. 6 (a) shows a representative example of such linear regression for one volunteer, in which MF decays over time with a linear fashion. The slope (negative) of the regression line was estimated as an indicator of myoelectric muscle fatigue. The average correlation coefficient of the linear fit over all the measurements was 0.86 ± 0.14 ($p = 0.01 \pm 0.05$).

The average decays of MF at different vibration frequencies were -2.0 ± 0.7 Hz/s, -2.3 ± 1.1 Hz/s, -2.5 ± 0.9 Hz/s, and -2.2 ± 0.9 Hz/s for 0 Hz, 20 Hz, 30 Hz, and 40 Hz, respectively. Fig. 7 (a, left) shows the normalized results. Our MF estimation indicates that vibration produces a larger degree of fatigue as compared to control condition (0 Hz). In particular, 30 Hz vibration seems to be the most fatiguing exercise. Our statistical analysis showed significant difference ($p < 0.05$) between 30 Hz and control condition.

Fig. 7. Normalized fatigue estimates for varying vibration frequencies: a) MF, b) CV, c) RMS, and d) FD. The asterisk indicates a significant difference ($p < 0.05$).

Similar results were found for the MF estimation without SP_{VF} removal, as shown in Fig. 7 (a, right).
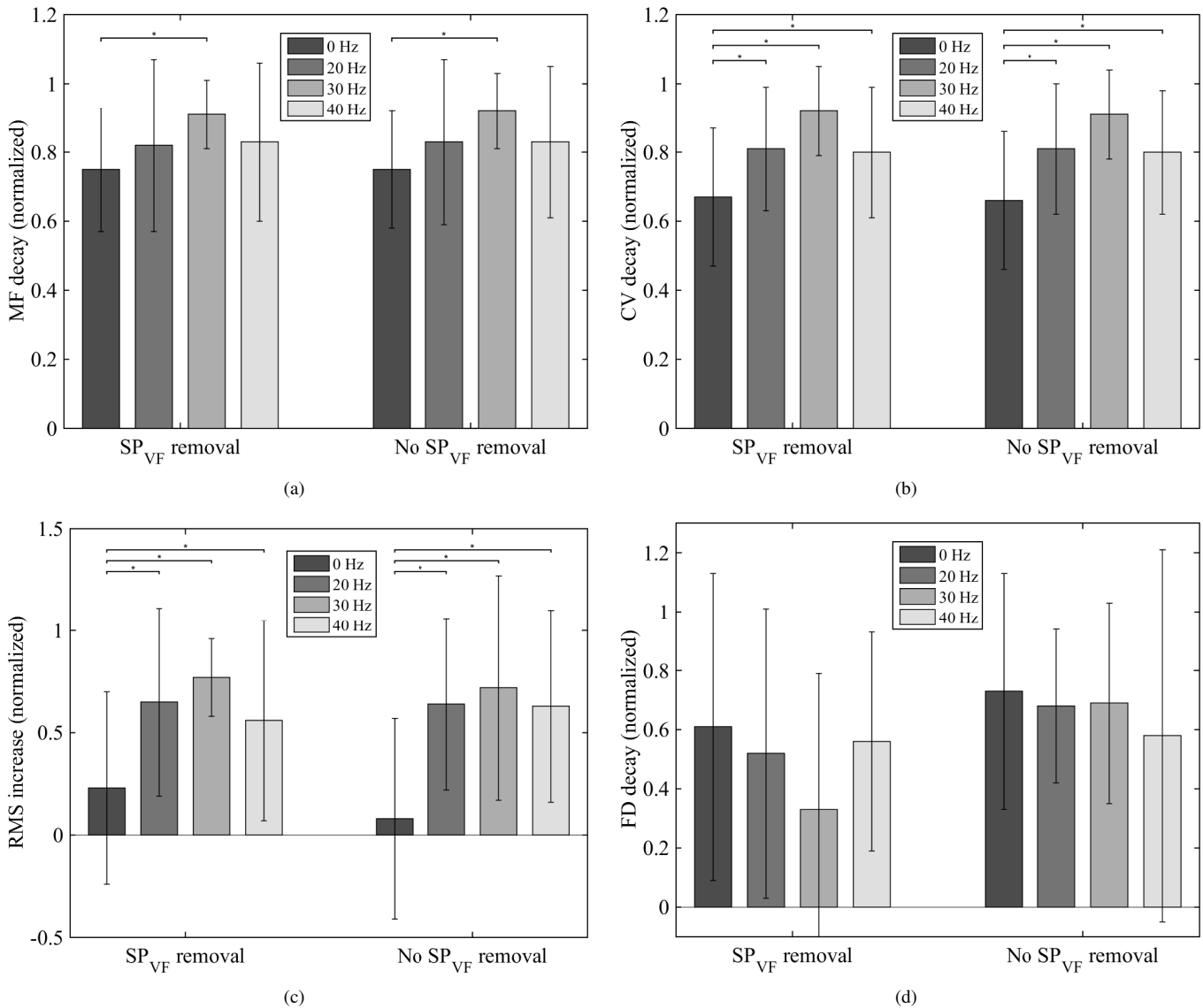
B. CV estimation

CV estimation with SP_{VF} removal revealed an average value of 3.58 ± 0.56 m/s, which is in line with the literature [45], [44], [50]. Fig. 5 (b) shows the initial CVs estimated at the first epoch of each dataset. Fig. 6 (b) shows the CV time evolution for one volunteer. Similar to the MF, the CV was found to decay over time with a linear fashion. The average correlation coefficient of the linear fit was 0.87 ± 0.14 ($p = 0.01 \pm 0.05$). The average decays of CV at different vibration frequencies were -0.050 ± 0.018 m/s^2, -0.063 ± 0.023 m/s^2, -0.074 ± 0.033 m/s^2, and -0.064 ± 0.037 m/s^2 for 0 Hz, 20 Hz, 30 Hz, and 40 Hz, respectively. The normalized results of CV decay are shown in Fig. 7 (b, left), which reveals the same fatiguing pattern for different vibration frequencies as observed in the MF estimation. CV estimation without SP_{VF}

removal has a similar trend, as shown in Fig. 7 (b, right).

C. RMS estimation

RMS estimation with SP_{VF} removal revealed an average value of 1.27 ± 0.58 mV. Different from the other three indicators, the RMS was found to increase over time, as shown in Fig. 6 (c). The average correlation coefficient of the linear fit was 0.51 ± 0.25 ($p = 0.20 \pm 0.26$), which is much lower than that of the MF and CV. The average increases of RMS were 10 ± 20 μV/s, 29 ± 25 μV/s, 34 ± 20 μV/s, and 30 ± 25 μV/s for 0 Hz, 20 Hz, 30 Hz, and 40 Hz vibration, respectively. Fig. 7 (c, left) shows the normalized results of RMS increase. The results suggested that vibration leads to larger RMS increase and, in particular, 30 Hz seems to produce the largest RMS increase. The difference between control condition and each vibration frequency was found to be significant ($p < 0.05$). Without SP_{VF} removal, a similar fatiguing effect was found for different vibration frequencies, as shown in Fig. 7 (c,

right).

D. FD estimation

After removing the SP_{VF}, an average value of 1.71 ± 0.03 was found for the FD over all the measurements, which is in the range reported in the literature [51]. Similar to the MF and CV, a linear decay of FD over time was also observed, as shown in Fig. 6 (d). However, the average correlation coefficient of the linear fit for the FD estimates (0.51 ± 0.25, $p = 0.20 \pm 0.30$) was much lower as compared to that of the MF and CV. The average decays at different vibration frequencies were -0.0039 ± 0.0032 /s, -0.0029 ± 0.0027 /s, -0.0023 ± 0.0023 /s, and -0.0033 ± 0.0025 /s for 0 Hz, 20 Hz, 30 Hz, and 40 Hz, respectively. The normalized results are shown in Fig. 7 (d, left). Our results indicate that vibration produces smaller FD decay as compared to control condition and, in particular, 30 Hz vibration seems to produce the smallest FD decay.

A different trend was found when the SP_{VF} was included in the analysis, as shown in Fig. 7 (d, right). FD decays obtained during vibration were smaller as compared to control condition. However, 30 Hz vibration resulted in the largest FD decay among all the vibration frequencies.

E. Mechanical fatigue

Mechanical fatigue was estimated as the relative drop in MVC measured after each task. Fig. 8 shows the normalized results of the fifteen subjects, in which the 30 Hz vibration is found to produce significantly ($p < 0.05$) larger MVC decay as compared to control condition.

IV. DISCUSSION

The effect of VE at different frequencies was investigated by analyzing mechanical fatigue (MVC decay) and myoelectric fatigue (MF, CV, RMS, and FD time evolutions) on the biceps brachii. For the EMG CV estimation, the ML method described in [36] was reported to have several advantages [37] and therefore adopted in the present study. All the CV estimates were between 2 and 6 m/s, in line with the values reported in the literature for this muscle [44], [45], [50]. Furthermore, in line with a number of authors [27], [47], a linear decay of CV over time (correlation coefficient > 0.8) was observed. In addition, for each subject, the CV estimates, similar to the MF estimates, showed small variations in their initial values estimated in different trials, suggesting the adopted 12-min rest interval to be sufficient for neuromuscular recovery.

It is extensively reported in the literature that sharp spectral peaks at the vibration frequency, SP_{VF}, can be observed in the EMG spectrum recorded during VE, whose interpretation (motion artifacts or muscle activity) remains controversial [2], [9], [14], [39], [40], [41]. In this study, a more thorough understanding of the fatiguing effect introduced by VE at different frequencies was pursued by fatigue estimation performed with and without SP_{VF} removal. The results obtained in both cases showed the same trend for the MF and CV, while
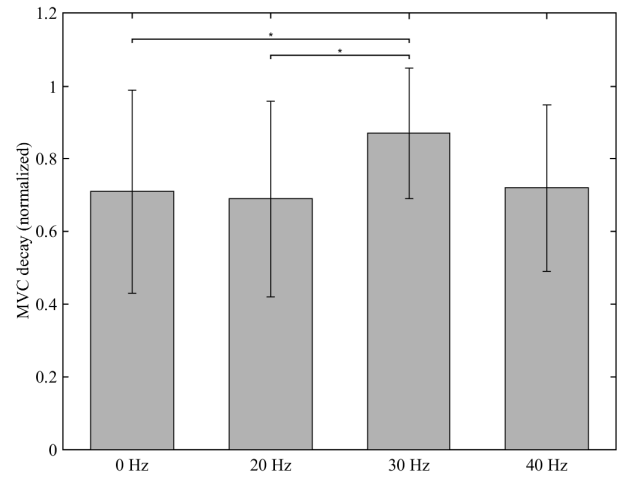

Fig. 8. Normalized MVC for varying vibration frequencies. The asterisk indicates a significant difference ($p < 0.05$).

slight differences were observed for the RMS and especially FD (Fig. 7).

A recent study has suggested that the CV, MF, and RMS are more sensitive to peripheral fatigue [29]. Therefore, our CV, MF, and RMS results suggest VE, especially at 30 Hz, to produce a larger degree of peripheral fatigue as compared to control condition. Previous work, directly applying mechanical vibration to the hand muscles, suggests that muscle peripheral fatigue develops at a higher rate under vibration, which has been ascribed to the effects of TVR [14], [21]. TVR results principally from an increase in motoneuron depolarization with the firing frequency of Ia-afferents, leading to a recruitment of motor unit of increasing threshold [14]. Motor unit fatigue resistance seems to decrease with increasing recruitment threshold [52]; it is therefore reasonable to expect a higher degree of fatigue under the effect of vibration.

Studies have also suggested that TVR increases with increasing vibration frequency up to 100 Hz [14]. However, in the present study, 30 Hz vibration was found to be the most peripherally fatiguing exercise. This may be explained by the complex vibration transmission chain in the adopted setup. It should be noted that the experimental setup in the present study is different from the one employed in [14]. Instead of applying mechanical vibration (displacement) directly to the muscle, our device provides force control, and vibration consists in the sinusoidal force modulation applied to the muscle. The generated force modulation is transmitted to the muscle via the bar, strap, handle, wrist, elbow, and muscle-tendon system, which introduces a mechanical low-pass filter dampening the transmission of high-frequency vibration to the muscle spindle, and therefore resulting in a decreased Ia-afferents driving.

Besides the involuntary reflex mechanism, studies have suggested that vibration may also have an effect on motor cortical excitability modulation [53]. Therefore, the vibration-induced fatiguing effect to the central nervous system should also be taken into consideration. In this study, the FD was estimated as an indicator for the central fatigue, as suggested by a recent study [29]. In ([29]), the FD was found to

decrease with increasing motor-unit synchronization, in *silico*, and during sustained contraction, in *in − vivo* [29]. Our FD estimation suggests vibration as a possible option to reduce central fatigue as compared to control condition.

Different from peripheral fatigue, the FD slopes estimated with and without SP_{VF} removal showed a different trend for 30 Hz vibration (Fig. 7 (d)). This may be explained by assuming the SP_{VF} component to mainly reflect muscle activity resulting from synchronization of a number of motor units through TVR. Indeed, our previous study indicated the SP_{VF} to be caused by vibration-induced stretch reflex rather than motion artifacts [40]. In this case, the motor-unit synchronization indicated by FD originates not only from the central nervous system but also from the TVR; removal of the SP_{VF} may therefore reduce the contribution of TVR-induced motor-unit synchronization, leading to a decrease in FD decay, particularly at 30 Hz. However, the assumption that FD is indicative of motor-unit synchronization is based on a simulation study [29], and the relation between FD decay and motor-unit synchronization increase should be studied more extensively. Furthermore, it should be noted that in this case, due to the calculation of the FD in the time domain, the SP_{VF} removal is performed by notch filtering, which may alter the spectrum of the signal.

In agreement with the analysis of myoelectric fatigue, estimation of mechanical fatigue revealed the largest MVC decay at 30 Hz. Among all the myoelectric fatigue indicators, the correlation coefficients of the linear fit for the RMSs and FDs over all epochs are much lower than those of the CVs and MFs; this result is in line with the literature [29], [47] and may due to the fact that the RMS and FD time course estimates are more scattered than both CV and MF. This findings suggest MF and CV decay to be the most reliable indicators for myoelectric fatigue. Moreover, the fatiguing effect of different vibration frequencies estimated by MF decay was in line with that estimated by CV decay (Fig. 7), further supporting the reliability of those two fatigue indicators. Indeed, the rate of change of MF and CV during a sustained contraction as indicative of muscle fatigue has been clearly established in the literature [26], [27].

V. CONCLUSION

In the present study, the relationship between vibration frequency and muscle fatigue during sustained contraction of the biceps brachii was investigated by using a fully controlled force-modulation VE setup. Both mechanical and myoelectric fatigue were estimated and their correlation was analysed. The results of our experiment suggest vibration exercise, especially at 30 Hz, to produce a larger degree of peripheral fatigue and a smaller degree of central fatigue as compared to control condition. These results indicates that such force-modulation VE system may achieve enhanced training effect (peripheral fatigue) while applying reduced load to the central nervous system, which may be particularly suited for rehabilitation programs. The results of this study may contribute to the analysis of VE and may motivate further research aiming at improving VE training protocols and introducing VE in rehabilitation programs.

APPENDIX A
ML METHOD

For the signal model in (2), assuming the noise in a single channel to be uncorrelated with the noise in the other channels, the multivariate Gaussian PDF can be expressed as

$$p(\underline{x}_{11}, ..., \underline{x}_{N_r N_c} | \theta, \underline{s}_c) = \prod_{c=1}^{N_c} \prod_{r=1}^{N_r} p(\underline{x}_{rc} | \theta, \underline{s}_c), \qquad (6)$$

where

$$p(\underline{x}_{rc} | \theta, \underline{s}_c) = \prod_{n=1}^{N} \frac{1}{\sqrt{2\pi}\sigma_{rc}} \exp\left[-\frac{\left(x_{rc}(n) - s_c[n - (r-1)\theta]\right)^2}{2\sigma_{rc}^2} \right].$$
$$(7)$$

Taking the logarithm of $p(\underline{x}_{11}, ..., \underline{x}_{N_r N_c} | \theta, \underline{s}_c)$, we obtain the following log-likelihood function,

$$\ln p(\underline{x}_{11}, ..., \underline{x}_{N_r N_c} | \theta, \underline{s}_c) = \text{constant} -$$
$$\frac{1}{2\sigma_{rc}^2} \sum_{c=1}^{N_c} \sum_{r=1}^{N_r} \sum_{n=1}^{N} \left(x_{rc}(n) - s_c[n - (r-1)\theta] \right)^2. \quad (8)$$

Differentiation of the log-likelihood function with respect to $s_c(n)$ yields

$$\frac{\partial \ln p(\underline{x}_{11}, ..., \underline{x}_{N_r N_c} | \theta, \underline{s}_c)}{\partial \underline{s}_c} =$$
$$\frac{1}{2\sigma_{rc}^2} \left(\sum_{r=1}^{N_r} 2x_{rc}[n + (r-1)\theta] - 2N_r s_c(n) \right). \quad (9)$$

By setting (9) to zero, the ML estimation of $s(n)$ is obtained by the average of the M channels aligned in time,

$$\hat{s}_c(n, \theta) = \frac{1}{N_r} \sum_{r=1}^{N_r} x_{rc}[n + (r-1)\theta]. \qquad (10)$$

Replacing $s_c(n)$ in (8) with $\hat{s}_c(n, \theta)$, the log-likelihood function can be expressed as

$$\ln p(\underline{x}_{11}, ..., \underline{x}_{N_r N_c} | \theta, \underline{s}_c) = \text{constant} -$$
$$\frac{1}{2\sigma_{rc}^2} \sum_{c=1}^{N_c} \sum_{r=1}^{N_r} \sum_{n=1}^{N} \left(x_{rc}(n) - \frac{1}{N_r} \sum_{m=1}^{N_r} x_{mc}[n + (m-r)\theta] \right)^2.$$
$$(11)$$

Omitting the factors that do not depend on θ, the multichannel ML estimator of θ is given by

$$\hat{\theta} = \arg\max_\theta \left(\sum_{c=1}^{N_c} \sum_{r=1}^{N_r} \sum_{n=1}^{N} \left[\frac{2}{N_r} \sum_{m=1}^{N_r} x_{rc}(n) x_{mc}[n + (m-r)\theta] \right. \right.$$
$$\left. \left. - \frac{1}{(N_r)^2} \left(\sum_{m=1}^{N_r} x_{mc}[n + (m-r)\theta] \right)^2 \right] \right). \quad (12)$$

Note that

$$\sum_{r=1}^{N_r} \Big(\sum_{m=1}^{N_r} x_{mc}[n+(m-r)\theta] \Big)^2$$
$$= \sum_{i=1}^{N_r} \Big(\sum_{r=1}^{N_r} \sum_{m=1}^{N_r} x_{rc}(n) x_{mc}[n+(m-r)\theta] \Big)$$
$$= N_r \Big(\sum_{r=1}^{N_r} \sum_{m=1}^{N_r} x_{rc}(n) x_{mc}[n+(m-r)\theta] \Big). \quad (13)$$

Inserting (13) into (12) we obtain

$$\hat{\theta} = arg\max_{\theta} \Big(\frac{1}{N_r} \sum_{c=1}^{N_c} \sum_{r=1}^{N_r} \sum_{m=1}^{N_r} \sum_{n=1}^{N} x_{rc}(n) x_{mc}[n+(m-r)\theta] \Big).$$
$$(14)$$

It turns out that the multichannel estimator averages all possible combination of pairwise cross-correlation functions and then finds the location of the maximum of the averaged function. However, since the signals $x(n)$ are only available for discrete values of θ, maximization of the averaged function results in a discrete estimation of the optimum θ, which depends on the sampling frequency. By using Parseval's equality, (14) can be transformed in the frequency domain, as given in (3). In (3), θ no longer needs to be constrained to integer values, but can be treated as continuous-valued.

REFERENCES

[1] C. Bosco, M. Cardinale, and O. Tsarpela, "Influence of vibration on mechanical power and electromyogram activity in human arm flexor muscles," *Eur J Appl Physiol*, vol. 79, no. 4, pp. 306–311, 1999.

[2] A. Abercromby, W. Amonette, C. Layne, and et al., "Variation in neuromuscular responses during acute whole-body vibration exercise," *Med Sci Sports Exerc*, vol. 39, no. 9, pp. 1642–1650, 2007.

[3] J. Rittweger, "Vibration as an exercise modality: how it may work, and what its potential might be," *Eur J Appl Physiol*, vol. 108, no. 5, pp. 877–904, 2010.

[4] M. Cardinale and C. Bosco, "The use of vibration as an exercise intervention." *Exerc Sport Sci Rev*, vol. 31, no. 1, pp. 3–7, 2003.

[5] M. Cardinale and J. Lim, "The acute effects of two different whole body vibration frequencies on vertical jump performance," *Med Sport*, vol. 56, no. 4, pp. 287–292, 2003.

[6] D. Cochrane and S. Stannard, "Acute whole body vibration training increases vertical jump and flexibility performance in elite female field hockey players," *Br J Sports Med*, vol. 39, pp. 860–865, 2005.

[7] S. S. Rees, A. J. Murphy, and M. L. Watsford, "Effects of whole-body vibration exercise on lower-extremity muscle strength and power in an older population: a randomized clinical trial," *Phys Ther*, vol. 88, no. 4, pp. 462–470, 2008.

[8] B. Poston, W. Holcomb, and M. Guadagnoli, "The acute effects of mechanical vibration on power output in the bench press," *J Strength Cond Res*, vol. 21, no. 1, pp. 199–203, 2007.

[9] M. Mischi and M. Cardinale, "The effects of a 28-hz vibration on arm muscle activity during isometric exercise," *Med Sci Sports Exerc*, vol. 41, no. 3, pp. 645–653, 2009.

[10] L. Xu, M. Cardinale, and et al., "8-week vibration training of the elbow flexorsby force modulation: effects on dynamic and isometric strength," *J Strength Cond Res*, 2015.

[11] M. Roelants, S. M. Verschueren, C. Delecluse, O. Levin, and V. Stijnen, "Whole-body-vibration-induced increase in leg muscle activity during different squat exercises," *J Strength Cond Res*, vol. 20, no. 1, pp. 124–129, 2006.

[12] G. Eklund and K. Hagbarth, "Normal variability of tonic vibration reflexes in man," *Exp Neurol*, vol. 16, no. 1, pp. 80–92, 1966.

[13] L. Bongiovanni, K. Hagbarth, and L. Stjernberg, "Prolonged muscle vibration reducing motor output in maximal voluntary contractions in man," *J Physiol*, vol. 423, no. 1, pp. 15–26, 1990.

[14] B. Martin and H. Park, "Analysis of the tonic vibration reflex: influence of vibration variables on motor unit synchronization and fatigue," *Eur J Appl Physiol Occup Physiol*, vol. 75, no. 6, pp. 504–511, 1997.

[15] C. Fromm and J. Noth, "Reflex responses of gamma motoneurones to vibration of the muscle they innervate," *J Physiol*, vol. 256, no. 1, pp. 117–136, 1976.

[16] D. Burke, K. E. Hagbarth, and et al., "The responses of human muscle spindle endings to vibration during isometric contraction," *J Physiol*, vol. 261, no. 3, p. 695711, 1976.

[17] Y. Hori, K. Hiraga, and S. Watanabe, "The effects of thiamylyl sodium on the tonic vibration reflex in man." *Brain Res*, vol. 497, pp. 291–295, 1989.

[18] P. Romaiguère, J. P. Vedel, J. P. Azulay, and S. Pagni, "Diferential activation of motor units in the wrist extensor muscles during the tonic vibration reflex in man." *J Physiol (Lond)*, vol. 444, pp. 645–667, 1991.

[19] J. M. Wakeling and A.-M. Liphardt, "Task-specific recruitment of motor units for vibration damping," *J Biomech*, vol. 39, no. 7, pp. 1342 – 1346, 2006.

[20] E. Ribot-Ciscar, C. Rossi-Durand, and J. Roll, "Increase muscle spindle sensitivity to movement during reinforcement manoeuvres in relaxed human subjects," *J Physiol*, vol. 523, no. 1, pp. 271–282, 2000.

[21] H. S. Park and B. J. Martin, "Contribution of the tonic vibration reflex to muscle stress and muscle fatigue," *Scand J Work Environ Health*, vol. 19, pp. 35–42, 1993.

[22] J. Wakeling and B. Nigg, "Modification of soft tissue vibrations in the leg by muscular activity," *J Appl Physiol*, vol. 90, no. 2, pp. 412–420, 2001.

[23] M. Cardinale and J. Lim, "Electromyography activity of vastus lateralis muscle during whole-body vibrations of different frequencies," *J Strength Cond Res*, vol. 17, no. 3, pp. 621–624, 2003.

[24] M. Cardinale and J. Rittweger, "Vibration exercise makes your musclesand bones stronger: fact or fiction?" *J Br Menopause Soc*, vol. 12, no. 1, pp. 12–18, 2006.

[25] L. Xu, C. Rabotti, and M. Mischi, "Novel vibration-exercise instrument with dedicated adaptive filtering for electromyographic investigation of neuromuscular activation," *IEEE Trans Neural Syst Rehabil Eng*, vol. 21, no. 2, pp. 275–282, 2013.

[26] L. Arendt-Nielsen, K. R. Mills, and A. W. Forster, "Changes in muscle fiber conduction velocity, mean power frequency, and mean EMG voltage during prolonged submaximal contractions," *Muscle Nerve*, vol. 12, no. 6, pp. 493–497, 1989.

[27] R. Merletti, M. Knaflitz, and C. J. D. Luca, "Myoelectric manifestations of fatigue in voluntary and electrically elicited contractions," *J Appl Physiol*, vol. 69, no. 5, pp. 1810–1820, 1990.

[28] T. Moritani, M. Muro, and A. Nagata, "Intramuscular and surface electromyogram changes during muscle fatigue," *J Appl Physiol*, vol. 60, no. 4, pp. 1179–1185, 1986.

[29] L. Mesin, C. Cescon, M. Gazzoni, R. Merletti, and A. Rainoldi, "A bi-dimensional index for the selective assessment of myoelectric manifestations of peripheral and central muscle fatigue," *J Electromyogr Kinesiol*, vol. 19, no. 5, pp. 851–863, 2009.

[30] K. C. McGill and L. J. Dorfman, "High-resolution alignment of sampled waveforms," *IEEE Trans Biomed Eng*, vol. 31, no. 6, pp. 462–468, 1984.

[31] I. Hunter, R. Kearney, and L. Jones, "Estimation of the conduction velocity of muscle action potentials using phase and impulse response function techniques," *Med Biol Eng Comput*, vol. 25, pp. 121–126, 1987.

[32] P. Lynn, "Direct on-line estimation of muscle fiber conduction velocity by surface electromyography," *IEEE Trans Biomed Eng*, vol. 26, pp. 564–571, 1979.

[33] D. Farina and F. Negro, "Estimation of muscle fiber conduction velocity with a spectral multidip approach," *IEEE Trans Biom Eng*, vol. 54, pp. 1583–1589, 2007.

[34] P. Parker and R. Scott, "Statistics of the myoelectric signal from monopolar and bipolar electrodes," *Med Biol Eng*, vol. 11, pp. 591–596, 1973.

[35] D. Farina, W. Muhammad, E. Fortunato, O. Meste, R. Merletti, and H. Rix, "Estimation of single motor unit conduction velocity from surface electromyogram signals detected with linear electrode arrays," *Med Biol Eng Comput*, vol. 39, pp. 225–236, 2001.

[36] D. Farina, M. Pozzo, E. Merlo, A. Bottin, and R. Merletti, "Assessment of average muscle fiber conduction velocity from surface EMG signals during fatiguing dynamic contractions," *IEEE Trans Biomed Eng*, vol. 51, no. 8, pp. 1383–1393, 2004.

[37] C. Rabotti, M. Mischi, S. G. Oei, and J. W. M. Bergmans, "Noninvasive estimation of the electrohysterographic action-potential conduction velocity," *IEEE Trans Biomed Eng*, vol. 57, no. 9, pp. 2178–2187, 2010.

[38] D. Farina and R. Merletti, "Methods for estimating muscle fibre conduction velocity from surface electromyographic signals," *Med Biol Eng Comput*, vol. 42, no. 4, pp. 432–445, 2004.

[39] A. Fratini, M. Cesarelli, P. Bifulco, and et al., "Relevance of motion artifact in electromyography recordings during vibration treatment," *J Electromyogr Kines*, vol. 19, no. 4, pp. 710–718, 2009.

[40] L. Xu, C. Rabotti, and M. Mischi, "On the nature of the electromyographic signals recorded during vibration exercise," *Eur J Appl Physiol*, vol. 115, pp. 1095–1106, 2015.

[41] R. Ritzmann, A. Kramer, M. Gruber, and et al., "EMG activity during whole body vibration: motion artifacts or stretch reflexes?" *Eur J Appl Physiol*, vol. 110, no. 1, pp. 143–151, 2010.

[42] L. Xu, C. Rabotti, and M. Mischi, "Characterization of a novel instrument for vibration exercise," in *Proc of the Annu Int Conf IEEE Eng Med Biol Soc*, Aug. 2012, pp. 2760–2763.

[43] R. Merletti, G. Balestra, and M. Knaflitz, "Effect of FFT based algorithms on estimation of myoelectric signal spectral parameters," in *Proc of the Annu Int Conf IEEE Eng Med Biol Soc*, Nov. 1989, pp. 1022–1023.

[44] W. Q. Li and K. Sakamoto, "The influence of location of electrode on muscle fiber conduction velocity and EMG power spectrum during voluntary isometric contraction measured with surface array electrodes," *Appl Human Sci*, vol. 15, no. 1, pp. 25–32, 1996.

[45] S. W. Davies and P. A. Parker, "Estimation of myoelectrc conduction velocity distribution," *IEEE Trans Biomed Eng*, vol. 34, no. 5, pp. 365–374, 1987.

[46] J. A. Gitter and M. J. Czerniecki, "Fractal analysis of the electromyographic interference pattern," *J Nrurosci Meth*, vol. 58, no. 12, pp. 103–108, 1995.

[47] R. Merletti, L. R. Conte, and D. Sathyan, "Repeatability of electrically-evoked myoelectric signals in the human tibialis anterior muscle," *J Electromyogr Kinesiol*, vol. 5, no. 2, pp. 67–80, 1995.

[48] H. W. Lilliefors, "On the kolmogorov-smirnov test for normality with mean and variance unknown," *J Am Stat Assoc*, vol. 62, no. 318, pp. 399–402, 1967.

[49] J. W. Tukey, "Comparing individual means in the analysis of variance," *Biometrics*, pp. 99–114, 1949.

[50] D. Farina and R. Merletti, "A novel approach for estimating muscle fiber conduction velocity by spatial and temporal filtering of surface EMG signals," *IEEE Trans Biomed Eng*, vol. 50, no. 12, pp. 1340–1351, 2003.

[51] V. Gupta, S. Suryanarayanan, and N. P. Reddy, "Fractal analysis of surface EMG signals from the biceps," *Int J Med Inform*, vol. 45, no. 3, pp. 185–192, 1997.

[52] J. A. Stephens and T. P. Usherwood, "The mechanical properties of human motor units with special reference to their fatiguability and recruitment threshold," *Brain Res*, vol. 125, no. 1, pp. 91–97, 1977.

[53] A. Fourment, J. M. Chennevelle, A. Belhaj-Saif, and B. Maton, "Responses of motor cortical cells to short trains of vibration," *Exp Brain Res*, vol. 111, no. 2, pp. 208–214, 1996.

Chiara Rabotti Chiara Rabotti received the M.Sc. degree in electrical engineering from the University of Florence, Italy, in 2004. In 2010 she received the Ph.D. degree from the Eindhoven University of Technology (TU/e) on the characterization of uterine activity during pregnancy. She is currently assistant professor at the Signal Processing Systems Group at the Electrical Engineering Department of the TU/e. Her research interests include biomedical signal processing and modeling with specific focus on electrohysterography, electromyography, and electrocardiography.

Massimo Mischi Massimo Mischi (SM10) received the M.Sc. degree in Electrical Engineering at La Sapienza University in Rome, Italy. In 2004 he received the Ph.D. degree from the Eindhoven University of Technology, the Netherlands. In 2007 he became assistant professor and since 2011 he is an associate professor at the Electrical Engineering Department of the Eindhoven University of Technology, where he chairs the Biomedical Diagnostics Research Lab. His research focuses on model-based quantitative analysis of biomedical signals. In 2011 he was awarded with a Starting Grant from the European Research Council (ERC) for his research on angiogenesis imaging. He is Senior Member of the IEEE and vice-chairman of the IEEE EMBS Benelux Chapter.

Lin Xu Lin Xu received the M.S. degree in electrical engineering from the University of Electronic Science and Technology of China, Chengdu, China, in 2010. He is currently a PhD candidate at the Eindhoven University of Technology, Eindhoven, Netherlands. His research interests include biomedical signal processing, with special emphasis on electromyography and neuromuscular conditioning.